10th Aachen Symposium on Signal Theory,
20-21 Sept. 20[redacted], pp 363-375

Radio Propagation Modelling and its Application for 3G Mobile Network Simulation

Ingo Forkel, Michael Salzmann

Communication Networks, Aachen University of Technology
Kopernikusstr. 16, D–52074 Aachen, Germany
Phone: +49 241 80 7915, E-mail: ifl@comnets.rwth-aachen.de

Abstract

For the simulation of mobile communication networks, like UMTS or HIPERLAN, it is necessary to model the radio channel accurately. The radio wave propagation modelling is the first estimate of the channel quality and hence, it experienced a lot of attraction in recent publications. This paper gives a comprehensive survey of propagation models and proves their applicability for mobile radio network environments. Especially the indoor, outdoor-to-indoor, and dense urban propagation characteristics are interesting in this context since high bit rate multimedia applications are expected to be used in such scenarios.

1 Introduction

For the simulation of wireless communication systems, such as the 3rd generation systems UMTS and HIPERLAN, it is important to model the radio channel's properties. One aim of these models is to get knowledge of the path loss between transmitters and receivers. Since an analytical description of path loss in complex scenarios is very difficult and computation time consumptive, appropriate models are needed, where mathematical approximations for the physical propagation mechanisms are defined. The efficiency and usability of these models are investigated in this paper.

An approved method to model radio wave propagation is ray tracing, which is based on geometrical optics and utilizes Snellius' law to determine reflections and transmissions and the *Uniform Theory of Diffraction* (UTD). The number of interactions such as reflections, transmissions and diffractions and the availability of computation resources limit the accuracy of the ray tracing method.

The results of simulations with the ComNets' ray tracing tool RaIn at typical frequencies (1.9 GHz and 5.2 GHz) are compared with the ones derived by means of different propagation models and statistically analyzed.

Sec. 2 gives an overview of the basic propagation mechanisms. In Sec. 3 various propagation prediction models for indoor and urban environments are discussed. In Sec. 4 the models' results are compared to the ones gained from ray tracing simulations. Furthermore, parameters fitted to several scenarios are presented.

2 Propagation Phenomena

The mechanisms which govern radio propagation in cellular systems are complex and diverse, but they can generally be attributed to the basic propagation mechanisms reflection, diffraction, and signal transmission through obstacles as illustrated in Fig. 1. Another effect which occurs in corridors, street canyons, and tunnels is wave-guiding. Due to their difficult modeling, wave-guiding effects are usually not considered.

Diffraction occurs when the radio path between the transmitter and receiver is obstructed by an impenetrable object. Based on Huygen's principle waves are formed e.g. around street corners so that radio waves can propagate through areas even though there is no *Line Of Sight* (LOS) path between transmitter and receiver.

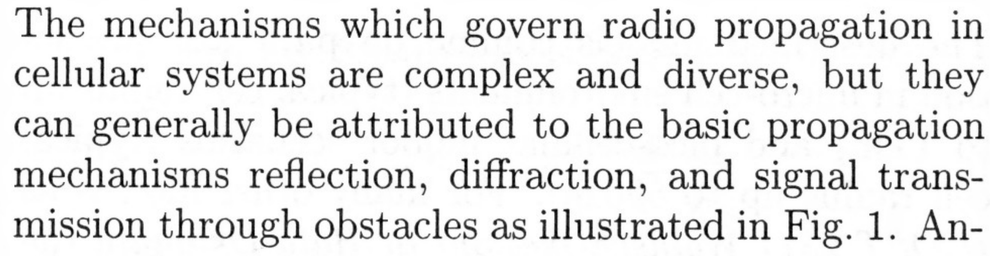

Figure 1: Basic propagation phenomena

There are differences in the propagation characteristics of in-building environments compared to outdoor environments. Radio propagation is usually more varied in indoor environments and depends on the architecture and construction of the building. This means that the particular type of building has a direct impact on the observed propagation characteristics. Furthermore, in most indoor environments only reflections and transmissions are dominant. Diffraction only contributes where reflected rays and rays transmitted through many walls are weaker than diffracted rays [1].

Basic propagation parameters are path loss and time dispersion. Time dispersion arises due to multi path propagation whereby replicas of the transmitted signal reach the receiver with different delays due to the propagation phenomena described above. Time dispersion determines the maximum data rate that may be transmitted without requiring equalization [2].

The focus in here is set on the analysis of path loss, which is defined as *the ratio of the effective transmitted power to the received power, calibrating out system losses, amplifier gains, and antenna gains* [3]. Various path loss prediction models were presented in journals and conference proceedings over the past years. A selection is presented in the following sections.

3 Propagation Models

The described models confine on path loss prediction in micro-cell environments (typical cell radius up to 1 km) and pico-cellular indoor scenarios (typical cell radius up to 500 m). For many other models as *(COST 231) Walfisch-Ikegami* or *Hata-Okumura* the parameters are not considered in a physically meaningful way for this cell types. Therefore the prediction error in these scenarios may be significantly large.

3.1 Free Space Propagation

The simplest propagation situation is free space propagation, where attenuation is related to the distance d between transmitter and receiver. Obstacles interfering the radio wave are not taken into account. With the wave length λ, the transmitted power P_T and antenna gains G_T and G_R the received signal power P_R results to

$$P_R(d) = P_T \cdot \left(\frac{\lambda}{4\pi d}\right)^2 \cdot G_T G_R \,. \tag{1}$$

With the definition of path loss where no antenna gains are considered this yields

$$\begin{aligned} L_F &= 10 \cdot \log \tfrac{P_T}{P_R} \\ &= 20 \cdot \log \left(\tfrac{4\pi \cdot d}{\lambda}\right) , \end{aligned} \tag{2}$$

which provides the free space path loss in dB.

3.2 One-Slope Model

In this simple model path loss is determined by the logarithmic distance and the power decay index n. Typical values for n are 2 for free space propagation (compare Eq. 2) and 3.5 - 6 in buildings, further values are presented in [2]. It is recommended to fit n to the particular scenarios. The *One-Slope* (OS) model is expressed by [4] as

$$L_{OS} = L_0 + 10\,n \cdot \log(d) \tag{3}$$

with

$L_0 = 20 \cdot \log\left(\frac{4\pi}{\lambda}\right)$, free space loss in 1 m distance,
n = power decay index,
d = distance between transmitter and receiver.

3.3 Dual-Slope Model

Micro cell measurements have indicated that path loss behaves different at close and distant ranges [5]. Therefore a *Dual-Slope* (DS) model as presented in [6] with

$$\begin{aligned} L_{DS_1}(d) &= 10 n_1 \cdot \log\left(\tfrac{4\pi d}{\lambda}\right) - a_0 \big|_{d<d_{Br}} \\ L_{DS_2}(d) &= L_{DS_1}(d_{Br}) + 10 n_2 \cdot \log\left(\tfrac{d}{d_{Br}}\right)\Big|_{d\geq d_{Br}} , \end{aligned} \tag{4}$$

where

n_1 = power decay index before d_{Br},
n_2 = power decay index beyond d_{Br},
d_{Br} = breakpoint distance,
a_0 = difference between L_{DS} and L_F at $d = 1$ m,

is more appropriate. The parameter a_0 is caused e.g. by wave guiding effects and varies between 0 dB and 5 dB. In the near region, the slope n_1 is set to 2. In the far region the slope is usually steeper with values of n_2 up to 6, as exemplarily shown in Fig. 2.

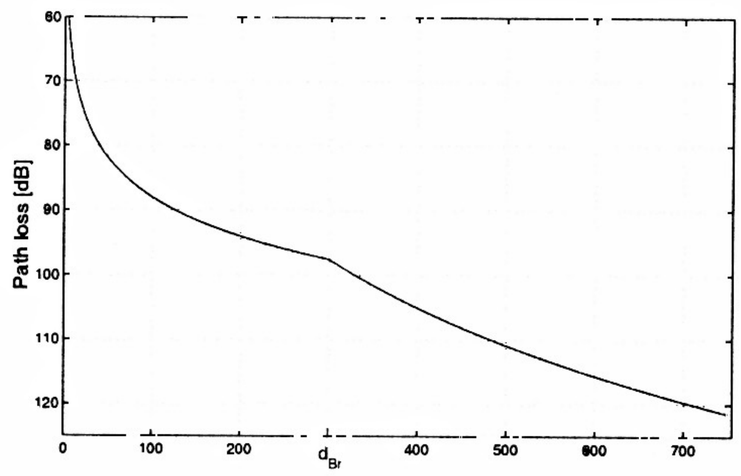

Figure 2: Dual slope model with $f = 1.9$ GHz

3.4 Multi-Wall Model

Another model especially for indoor radio propagation presented in [4] is the *Multi-Wall* (MW) model, which gives the indoor path loss as the free space loss

added with losses for the walls and floors penetrated by the *Line Of Sight* (LOS) between transmitter and receiver. Path loss is given by

$$L_{MW} = L_F + L_C + \sum_{i=1}^{I} k_{w_i} L_{w_i} + k_f^{\left[\frac{k_f+2}{k_f+1} - b\right]} \cdot L_f \quad (5)$$

with the parameters

L_F = free space loss as defined in Eq. 2,
L_C = constant loss,
I = number of wall types,
k_{w_i} = number of penetrated walls of type i,
L_{w_i} = loss of wall type i,
k_f = number of penetrated floors,
b = empirical parameter,
L_f = loss between adjacent floors.

In [7] a simplified version of the MW model is proposed for UMTS indoor office test environments. Within a floor path loss is calculated by a one-slope model, the losses due to floors are given through the same expression as in Eq. 5. With values of b=0.46 and L_C=37 dB path loss results to

$$L_{MW}^{(30.03)} = 37 + 30\log(d) + 18.3\, k_f^{\left[\frac{k_f+2}{k_f+1} - 0.46\right]}. \quad (6)$$

3.5 Keenan-Motley Model

A similar model is the *Keenan-Motley* (KM) model presented in [8] as

$$L_{KM} = S + 10\, n \cdot \log(d) + k_f \cdot F, \quad (7)$$

that enhances the one-slope model with the introduction of a term F similar to L_F, which takes the penetration loss of floors into account. S is the real path loss at 1 m unlike L_0, the free space loss.

Keenan and Motley propose f=16 dB, S=21 dB, and n=3.5 for a frequency of 1700 MHz.

3.6 Multi-Wall-and-Floor Model

A more sophisticated model is described in [9]. The *Multi-Wall-and-Floor* (MWF) model considers the fact that the walls' (and floors') penetration losses differ for each precedingly traversed wall (or floor, respectively). Path loss is calculated by

$$L_{MWF} = L_{OS} + \sum_{i=1}^{I} \sum_{k=1}^{k_{w_i}} L_{w_{ik}} + \sum_{j=1}^{J} \sum_{k=1}^{k_{f_j}} L_{f_{jk}}, \quad (8)$$

where

L_{OS} = one slope loss as given in Eq. 3,
k_{w_i} = number of traversed walls of category i,
$L_{w_{ik}}$ = loss due to wall type i and k^{th} traversed wall,
J = number of floor types,
k_{f_j} = number of traversed floors of category j,
$L_{f_{jk}}$ = loss due to floor type j and k^{th} traversed floor.

Several model parameters are given in [9]. Sec. 4.2 introduces the parameters of the MWF model for application in indoor environments at 1.9 GHz.

3.7 Berg Model

For outdoor path loss calculations along streets surrounded by buildings which are considerably taller than the height of the antennas, the following Berg model is proposed in [10].

Along street s_0 the signal seems to originate from the actual transmitter location. The received signal strength along a perpendicular street behaves as if the wave originates from a virtual transmitter located in the proximity of the street crossing. Between these two extreme cases the model generates a continuous path loss as a function of the angle θ.

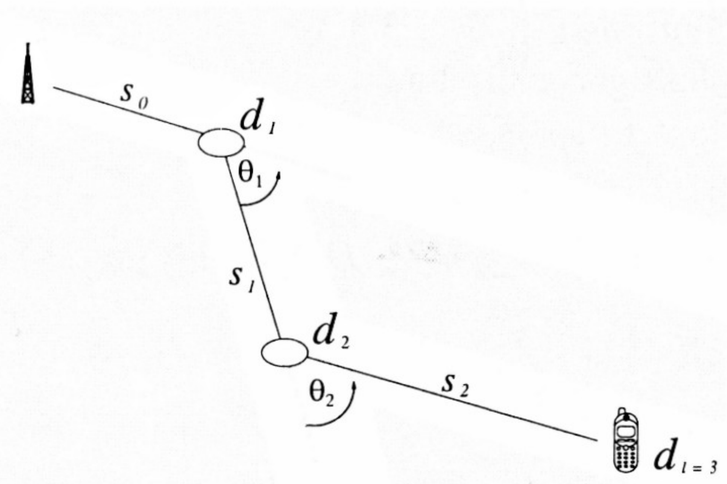

Figure 3: Example of street orientation

Similar to Eq. 2 path loss is determined by

$$L_{Berg} = 20 \cdot \log\left(\frac{4\pi d_l}{\lambda}\right), \quad (9)$$

where l is the number of single street elements along the path from transmitter to receiver. The 'illusory' distance d_l is defined by the recursive expressions

$$\begin{aligned} k_m &= k_{m-1} + d_{m-1} \cdot q_{m-1} \\ d_m &= k_m \cdot s_{m-1} + d_{m-1} \end{aligned} \quad (10)$$

with the initial values k_0=1 and d_0=0. In Fig. 3 the solid line describes the track of a propagating wave along a m=3 segment path. The value s_m is the physical distance between nodal points, d_m is the 'illusory' distance defined in Eq. 10, and m is the number of sections between the nodal points included in the calculation. The parameter q_m determines the angle dependence of the path loss. As a simple approach to model the angle dependence of q_m, Berg proposes the expression

$$q_m(\theta_m) = \left(q_{90^\circ} \cdot \frac{\theta_m}{90}\right)^{\nu}, \quad (11)$$

where ν determines the shape of the function. Possible parameters are q_{90°=0.5 and ν=1.5.

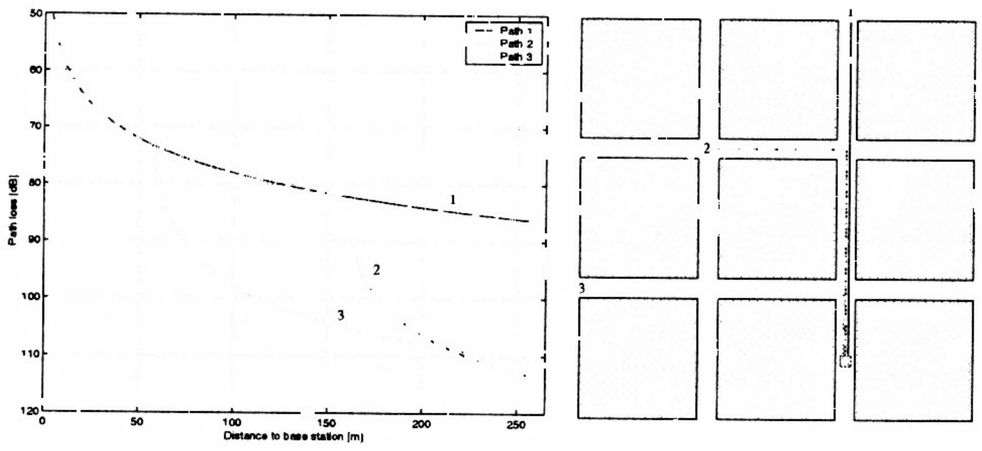

Figure 4: Path loss calculation with Berg's model

Fig. 4 shows an example path loss plot calculated for three different paths in a Manhattan like urban scenario as described in Sec. 4.3. Path one is a LOS path, path two contains a crossing after 57.5 m and path three bends of after 165 m.

As mentioned in Sec. 3.3 the distance dependence of path loss generally has a dual slope behavior. Due to this fact Eq. 9 is extended to

$$L_{Berg} = 20 \cdot \log\left[\frac{4\pi d_1}{\lambda} D\left(\sum_{j=1}^{m} s_{j-1}\right)\right], \qquad D(x) = \begin{cases} \frac{x}{d_{Br}} & \text{for } x > d_{Br} \\ 1 & \text{for } x \le d_{Br} \end{cases}. \tag{12}$$

In [7] a value of d_{Br}=300 m is proposed for UMTS.

3.8 Outdoor to Indoor Propagation

In the chapter 'Building Penetration' of [4], Berg presents an outdoor to indoor propagation model that takes into consideration the angle of incidence of a wave, penetrating a building wall. This model is based on measurements in the frequency range 900–1800 MHz at distances up to 500 m. The total path loss is determined by

$$L = 32.6 + 20\log(f) + 20\log(S+d) + W_e + W(\theta) + \max(\Gamma_1, \Gamma_2), \tag{13}$$

with the parameters (compare Fig. 5)

f = frequency,
S = distance between transmitter and the external wall,
W_e = external wall loss at perpendicular penetration,
$W(\theta) = WG_e \cdot (1-\sin(\theta))^2$, angle dependent loss,
WG_e = additional loss in external wall if $\theta = 0°$,
$\Gamma_1 = W_i \cdot k_w$,
W_i = loss in the internal walls,
k_w = number of penetrated walls,
$\Gamma_2 = \alpha \cdot (d-2) \cdot (1-\sin(\theta))^2$.

The following parameter values are recommended in the model:

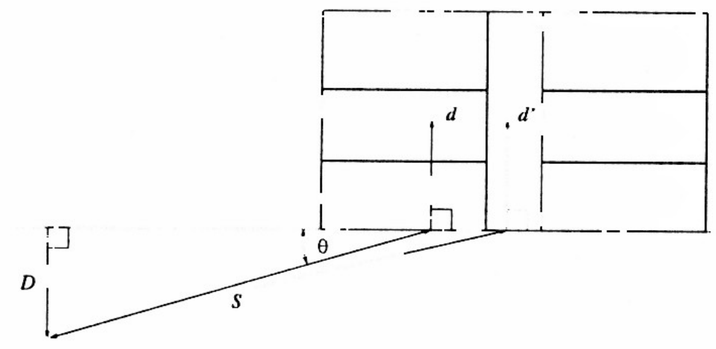

Figure 5: Outdoor to indoor propagation at angular incidence of a wave

W_e = 4 -10 dB, (concrete with windows 7 dB, wood 4 dB)
W_i = 4–10 dB, (concrete 7 dB, wood and plaster 4 dB)
WG_e = about 20 dB
α = about 0.6 dB/m

The wall loss is not necessarily the physical loss, it is the loss that gives reasonable agreement when the model is applied and includes other obstacles in the building. Depending on the environment considerably greater values can occur.

4 Model Evaluation

4.1 Ray Tracing

Ray tracing methods are based on geometrical optics where objects have dimensions that are much larger than the wave length and where electromagnetic waves are assumed as rays. Rays are followed until they hit an object. At this location, a reflected or transmitted ray is initiated. The new ray's direction is determined by Snellius' law. Diffracted rays can be considered by means of the UTD [11]. Rays are homogeneously emitted from a unit sphere centered at the transmitter location and all regions are covered evenly by rays. The reflection and transmission characteristics of the objects, e.g. a room wall, are determined by their geometric measures and the complex dielectric permittivity ε, which varies with the frequency of the transmitted signal. Rays that intersect an imaginary detection area around the receiver, the reception sphere, after a number of reflections, transmissions, and diffractions account to the received signal.

Ray tracing simulations require a very accurate data base for both, the geometry of the scenario and the material parameters. Furthermore, computation time increases with the number of interactions between rays and objects. Therefore, in mobile radio simulation tools other path loss prediction methods are needed to analyze large scenarios with many mobile stations.

Further information on the ray tracing algorithms used can be found in [12], a general introduction to ray tracing is given in [13].

4.2 Pico-Cells (Indoor Environment)

Typical Office Scenario

The properties of indoor radio propagation were analyzed in two scenarios. The office scenario shown in Fig. 6 is very similar to the one proposed in [7], but was extended by meeting rooms. The floor height amounts to 3 m. The concrete walls are 15 cm thick, windows and doors are not specified to keep the ray tracing results more general and exclude special cases like basestation positions in direct proximity to doors and windows.

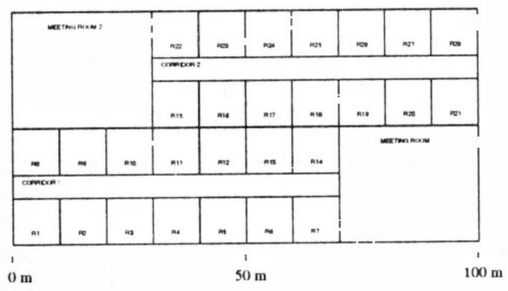

Figure 6: Indoor office scenario

Ray tracing simulations have been performed for different rooms with up to three penetrated walls. The influence of penetrated floors in multi storey buildings was not investigated.

In each one of the analyzed rooms the number of walls traversed by the path from the particular basestation to the receiver is constant. This allows an application of the MWM and the MWF model over the whole room area instead of determining the number of penetrated walls for each evaluated receiver position.

Tab. 1 shows the result of a comparison between the One-Slope model and ray tracing. In a first approach the slope n was set to 3.7, a value often referenced in literature [7]. An adaptation of n to the particular conditions leads to a reduced deviation of modeled path loss from ray tracing results, but the *STandard Deviation* (STD) remains at about 6 dB for 1.9 GHz and 11 dB for 5.2 GHz.

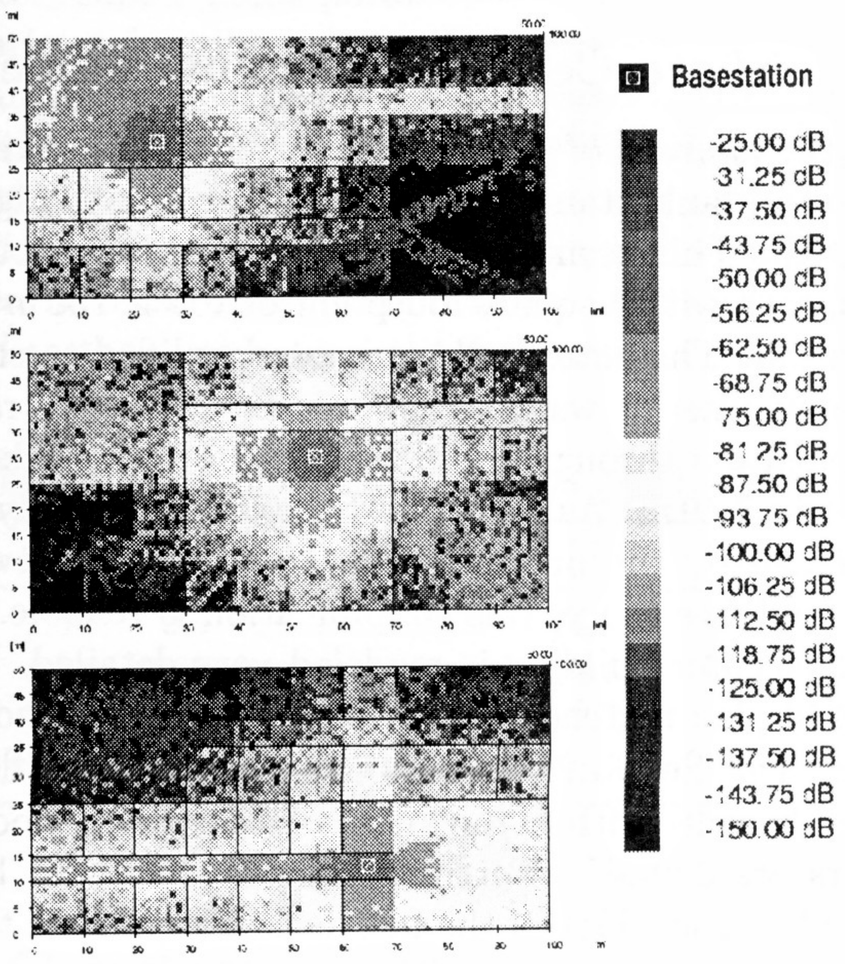

Figure 7: Ray tracing results for the three analyzed basestation locations

Table 1: One-Slope model (f=1.9 GHz)

BS position	n	Mean Deviation [dB]	STD [dB]
Large Room	3.7	1.337	6.160
Small Room	3.7	2.171	7.470
Corridor	3.7	3.565	7.547
Large Room	3.82	0.03	6.040
Small Room	3.87	0.00	7.273
Corridor	4.00	0.08	7.161

Table 2: Multi-Wall model (f=1.9 GHz)

Basestation position	L_w [dB]	STD [dB]
Large Room	11.45	4.557
Small Room	11.86	5.772
Corridor	12.08	5.313

Table 3: Multi-Wall-and-Floor model (f=1.9 GHz)

BS position	L_{w11}	L_{w12}	L_{w13}	STD [dB]
Large Room	13.39	12.44	8.53	5.45
Small Room	12.99	12.08	8.01	5.50
Corridor	12.30	10.90	8.78	4.39

Table 4: Multi-Wall-and-Floor model (f=5.2 GHz)

BS position	L_{w11}	L_{w12}	L_{w13}	STD [dB]
Large Room	22.50	22.65	19.40	5.26
Corridor	30.69	23.20	19.35	5.08

A reduced deviation can be achieved by using the MWM. For Tab. 2, the parameter L_w was chosen in a way that the mean difference between the path loss values gained from the model and ray tracing results disappears. The parameter L_C was set to 0.

A further improvement can be achieved by using the MWF model which allows to set the wall loss in dependence to the order of the traversed walls. With the performance of the models the effort of gaining parameters increases. Without a detailed knowledge of the scenario a reasonable usage of the MWF model is not possible. With the parameters given in Tab. 3 the mean deviation in each analyzed room is below 0.01 dB. The MWF parameters derived from the ray tracing simulations are in good accordance with the parameters presented in [9]. The wall loss tends to decrease with each traversed wall. As the only one of the analyzed models the MWF model is capable to consider inhomogenities in the scenario as stronlgy varying room sizes and changing wall materials. Tab. 4 presents the results for radio propagation at 5.2 GHz.

Real Office Scenario

Another analyzed scenario is a model of a corridor in the Helmholtzgebäude of the TU Ilmenau (see Fig. 8). The stone walls are 24 cm thick and the floors heigth is 3.17 m.

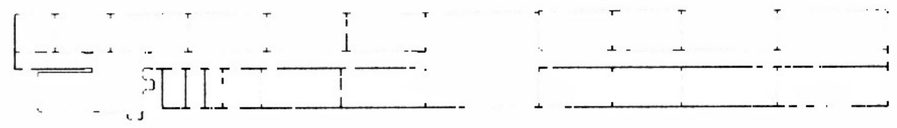

Figure 8: Real office scenario (Helmholtz building at TU Ilmenau)

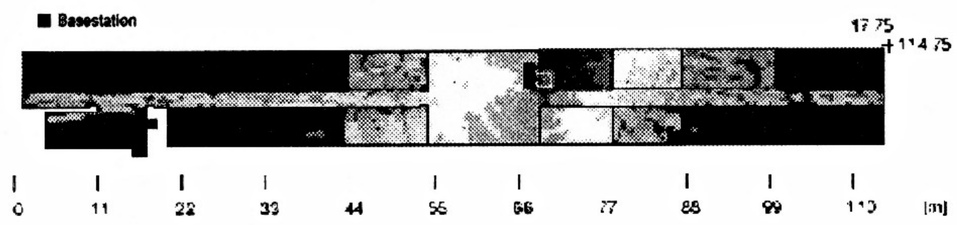

Figure 9: Ray tracing result for 1.9 GHz with obstacle

The analyzed indoor scenario does not have other obstacles as walls and doors except a soda machine situated in the central hall, as is common in office buildings. This machine is modeled by a steel plate box marked by the dark rectangle in Fig. 9. The influence of the obstacle on propagation is evident. In the segment behind the machine path loss shows clearly increased values.

Fig. 10 shows a comparison of two path loss plots at the frequencies 1.9 GHz and 5.2 GHz for the real office scenario. The attenuation due to the first wall is above average high. The MWF model with its different parameters for the two walls can take this fact into account and performs significantly better compared to the One-Slope model and the MWM.

Path loss at 5.2 GHz is much stronger than at 1.9 GHz. This fact is based on the general frequency dependence of path loss (mind the ordinates' scale in Fig. 10).

Table 5: Parameters for office scenario (f = 1.9 GHz)

Model	Parameters	STD [dB]
OS	n=6.16	6.70
MWM	L_w=34.0 dB, L_c=0	10.37
MWF	L_{w11}=44.0 dB, L_{w12}=16.6 dB, n=2	5.84

Table 6: Parameters for office scenario (f = 5.2 GHz)

Model	Parameters	STD [dB]
OS	n=9.05	11.43
MWM	L_w=56.9 dB, L_c = 0	12.01
MWF	L_{w11}=69.6 dB, L_{w12}=35.4 dB, n=2	5.66

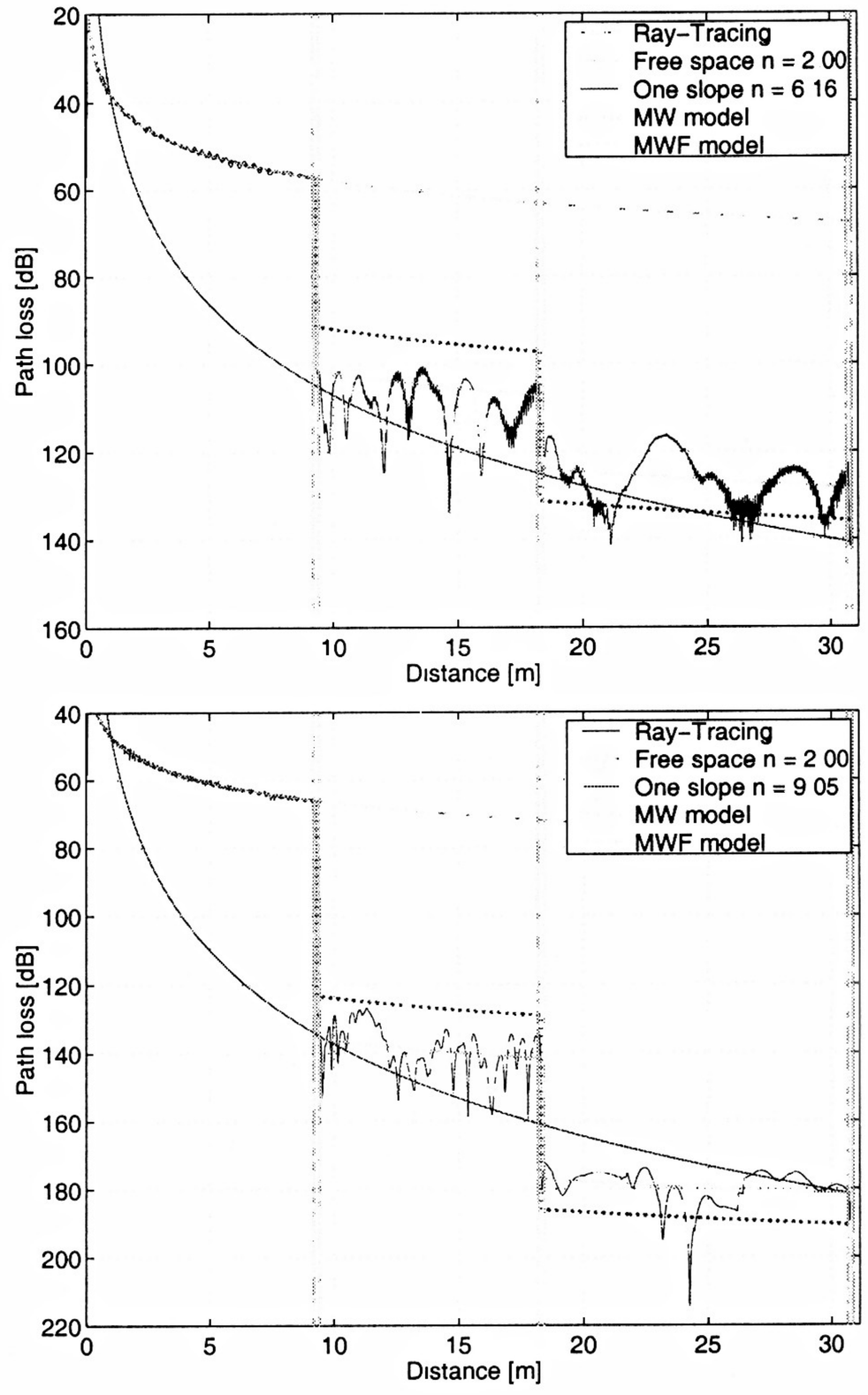

Figure 10: Comparison of path loss plots for real office scenario at 1.9 GHz (upper plot) and 5.2 GHz (lower plot)

4.3 Micro-Cells (Urban Environment)

For the analysis of propagation in an urban environment, a Manhattan like scenario according to Fig. 11 is used. This scenario consists of nine office buildings, each with a square footpoint of 100 × 100 m and 12 m tall. The outer buildings are simplified to cubes without interior walls and windows. To avoid radio propagation through these blocks, the wall thickness is set to 2.49 m. As reflection behaviour is mainly determined by the properties of the interface between wall and free space, this simplification is reliable.

The center building is modeled very detailed. The ground plan matches the doubled indoor scenario explained in Sec. 4.2. In every one of the four floors interior walls with a thickness of 15 cm and wooden doors are defined. Further obstacles have not been added. About 65 % of the facade consist of 1 cm thick single glassed windows. The exterior concrete walls are 27 cm thick.

The comparison of ray tracing results with path loss

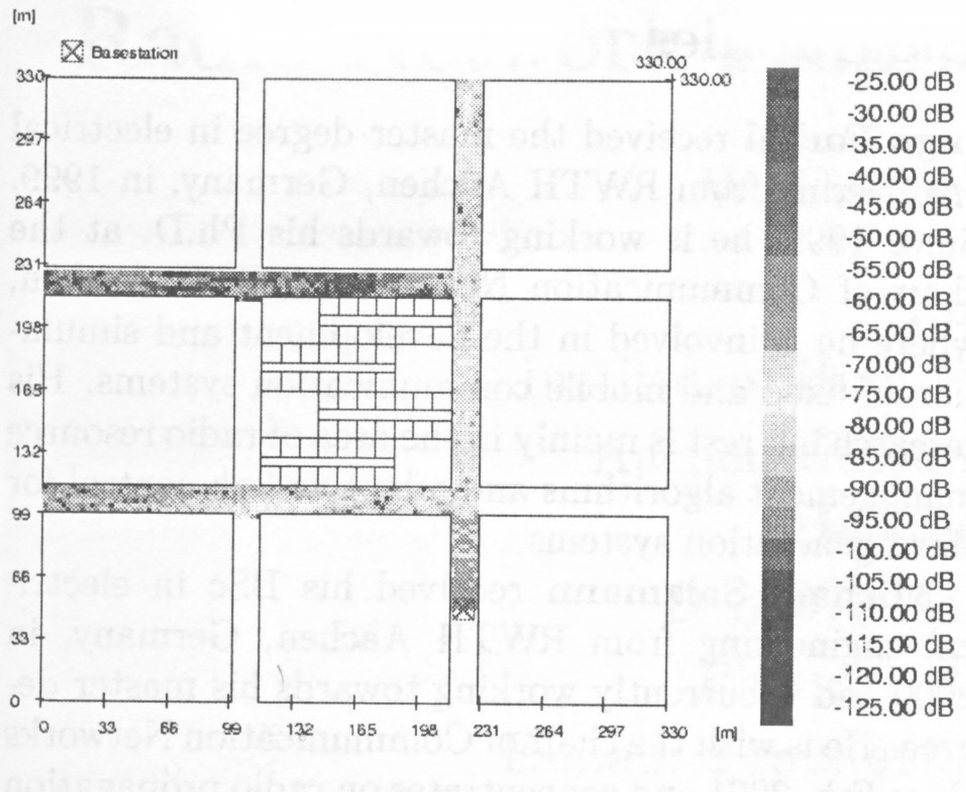

Figure 11: Ray tracing result for urban scenario at 1.9 GHz

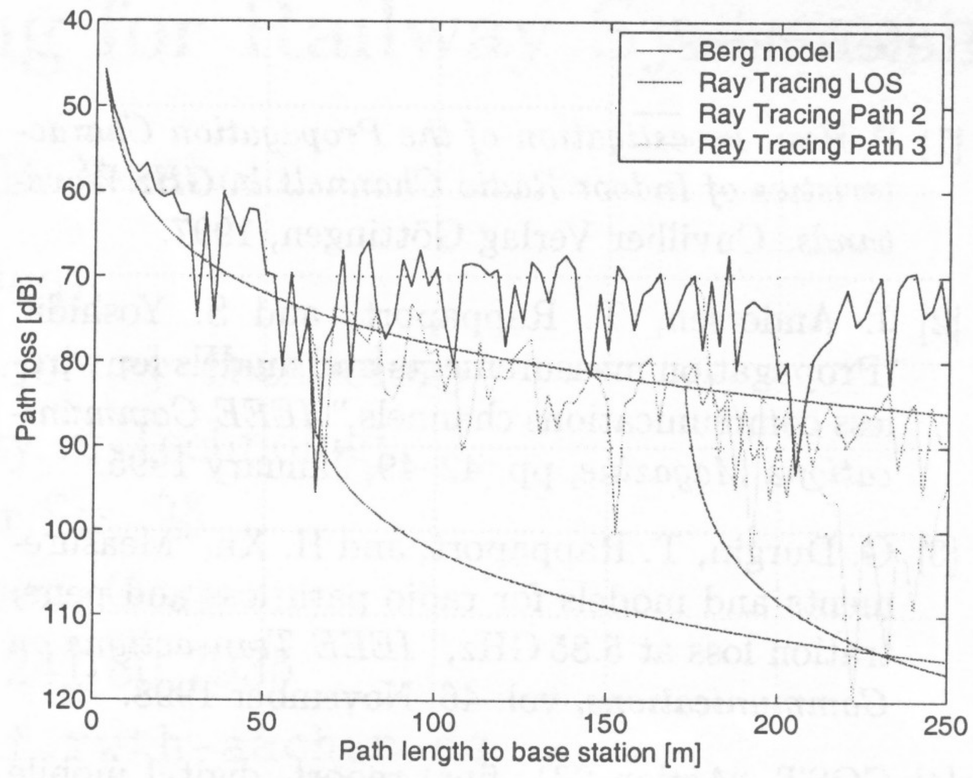

Figure 12: Berg model as proposed in [7]

values gained from the Berg model shows that using the model with standard parameters as proposed in [7, 10] does not yield completely satisfactory results as illustrated in Fig. 12.

Due to wave guiding effects in the street canyons the path loss increases less with the distance as assumed in [10], where the slope was set to a fixed value of 2, which correponds to free space propagation. To take this wave guiding effect into consideration, the Berg model was extended by a new parameter n to vary the slope. Therefore, Eq. 9 is changed according to

$$L_{Berg} = 10n \cdot \log\left(\frac{4\pi d_l}{\lambda}\right) . \qquad (14)$$

Fig. 13 shows the comparison of the modified Berg model with optimized parameters to the ray tracing results. Tab. 7 holds parameters fitted to the urban scenario as described above. From these results, a significantly lower value for q as proposed in [10] should be used. Moreover, at least a two-fold adaptation of q depending on the distance between transmitter and building corner is recommended since the path loss values increase faster after the second corner compared to the ones behind the first corner.

Table 7: Berg Model Parameters (f=1.9 GHz)

n	ν	q	Mean Deviation [dB]	STD [dB]
2	1.5	0.5	- 14.98	11.08
2	1.5	0.63	-16.11	11.59
2	1.5	0.1	-7.78	7.79
1.8	1.5	0.14	0.00	7.62

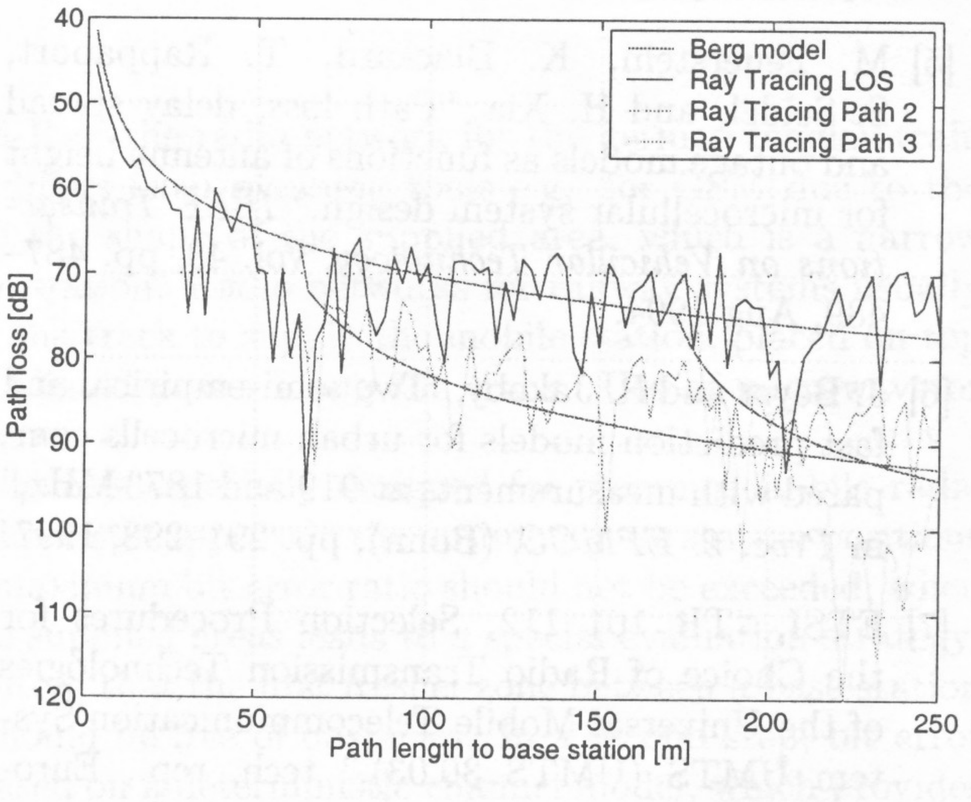

Figure 13: Extended Berg model with optimized parameters

5 Conclusion

Various path loss models are presented and their applicability for radio communication networks is proven by comparison with ray tracing results. Therefore, different models are optimally parameterized and the resulting deviation to the simulation results are presented. With carefully defined parameters all the models seem to provide reliable attenuation values to be used in system level simulations of communication networks.

A further comparison of the propagation model results with radio signal strength measurements in real environments should fine-tune the required parameters and improve modelling accuracy.

Acknowledgement

The authors like to thank Prof. B. Walke and Matthias Lott for their helpful advice to this work. The contributions of Peter Seidenberg and Stefan Krämer are highly appreciated.

References

[1] P. Hou, *Investigation of the Propagation Characteristics of Indoor Radio Channels in GHz Wavebands.* Cuvillier Verlag Göttingen, 1997.

[2] J. Andersen, T. Rappaport, and S. Yoshida, "Propagation measurements and models for wireless communications channels," *IEEE Communications Magazine*, pp. 42 -49, January 1995.

[3] G. Durgin, T. Rappaport, and H. Xu, "Measurements and models for radio path loss and penetration loss at 5.85 GHz," *IEEE Transactions on Communications*, vol. 46, November 1998.

[4] COST, "Action 231, final report, digital mobile radio towards future generation systems," tech. rep., European Commission, Brussels, 1999.

[5] M. Feuerstein, K. Blackard, T. Rappaport, S. Seidel, and H. Xia, "Path loss, delay spread and outage models as functions of antenna height for microcellular system design," *IEEE Transactions on Vehicular Technology*, vol. 43, pp. 487–489, Aug 1994.

[6] J. Beyer and R. Jakoby, "Two semi-empirical and fast prediction models for urban microcells compared with measurements at 919 and 1873 MHz," in *Proc. 2. EPMCC*, (Bonn), pp. 291–298, 1997.

[7] ETSI, "TR 101 112, Selection Procedures for the Choice of Radio Transmission Technologies of the Universal Mobile Telecommunication System UMTS (UMTS 30.03)," tech. rep., European Telecommunications Standards Institute, Apr. 1998.

[8] A. Motley and J. Keenan, "Personal communication radio coverage in buildings at 900 MHz and 1700 MHz," *Electronic Letters*, vol. 24, June 1988.

[9] M. Lott and I. Forkel, "A multi-wall-and-floor model for indoor radio propagation," in *Proc. VTC 2001 Spring*, IEEE, May 2001.

[10] J. Berg, "A recursive method for street micro-cell path loss calculations," in *Proc. PIMRC 1995*, vol. 1, pp. 140–143, 1995.

[11] R. Kouyoumijan and P. Pathak, "A uniform geometrical theory of diffraction for an edge in a perfectly conducting surface," *Proceedings of the IEEE*, vol. 62, pp. 1448–1461, Nov. 1974.

[12] M. Lott, "On the performance of an advanced 3D ray tracing method," in *Proc. of European Wireless & ITG Mobile Communication*, 1999.

[13] A. Glassner, *An Introduction to Ray Tracing.* Academic Press, 1989.

Biographies

Ingo Forkel received the master degree in electrical engineering from RWTH Aachen, Germany, in 1999. Since 1999, he is working towards his Ph.D. at the chair of Communication Networks, RWTH Aachen, where he is involved in the development and simulation of fixed and mobile communication systems. His research interest is mainly in the area of radio resource management algorithms and adaptive link control for third generation systems.

Michael Salzmann received his BSc in electrical engineering from RWTH Aachen, Germany, in 2000 and is currently working towards his master degree. He is with the chair of Communication Networks since Feb. 2001 and concentrates on radio propagation modelling for the next generation communication networks.